Journal of Molecular Structure 1189 (2019) 181–186

Contents lists available at ScienceDirect

Journal of Molecular Structure

journal homepage: http://www.elsevier.com/locate/molstruc

Effect of loading and standbye time of the organic dye N719 on the photovoltaic performance of ZnO based DSSC

Seval Aksoy [a], Kamuran Gorgun [b], Yasemin Caglar [c], Mujdat Caglar [c, *]

[a] Department of Physics, Faculty of Science, Sinop University, Sinop, Turkey
[b] Department of Chemistry, Faculty of Arts and Science, Eskisehir Osmangazi University, Eskisehir, 26480, Turkey
[c] Department of Physics, Faculty of Science, Eskisehir Technical University, Eskisehir, 26470, Turkey

ARTICLE INFO

Article history:
Received 21 February 2019
Received in revised form
3 April 2019
Accepted 9 April 2019
Available online 10 April 2019

Keywords:
ZnO nanopowders
Microwave assisted hydrothermal
DSSC

ABSTRACT

In this work, ZnO nanopowders were synthesized by microwave assisted hydrothermal method. To measure the photoelectrochemical properties of the obtained ZnO nanopowders, ZnO film was coated on FTO by using doctor blade method and the dye solution consisting N719 was used. For the investigations of structural and morphological properties, X-ray diffraction (XRD) measurements and scanning electron microscopy (SEM) analysis were carried out. The optical reflectance of the ZnO films with and without dye were recorded using spectrophotometer and by using Kubelka-Munk function, the two optical band gaps were detected at about 3.25 eV (direct band gap of ZnO) and 2.20 eV. The current–voltage (I–V) characterizations of fabricated ZnO-DSSCs were performed for three consecutive days and the best performance was obtained from the cell at 2 h loading time and 2 day standbye time, with their photovoltaic parameters were the J_{sc} of 1.62 mAcm^{-2}, V_{oc} of 0.64 V, FF of 0.62, and $n\%$ of 0.64%, respectively.

1. Introduction

The fact that the sun is a constant source of energy has enabled us to benefit from its energy by converting it into heat and electric energy. In today's conditions, technological and scientific changes in the world have made solar energy popular and electricity production from it. Dye sensitized solar cells (DSSCs) are important devices because they respond to many environmental and energy problems. DSSC is one of the most promising candidates for achieving efficient solar energy conversion because it is flexible, inexpensive and easy to manufacture. In the years to come, dye sensitized solar cells (DSSCs), an alternative energy source is expected to increase its contribution to overall energy production [1]. DSSC, also known as Graetzel cells, was first discovered in 1988 by M. Graetzel and Brian O'Regan [2] in UC Berkley and subsequently developed by the same individuals in 1991 at the École Polytechnique Fédéralede in Lausanne (EPFL).

In the early 1970s, TiO_2 from photoelectrochemical cells was found to split water with small bias voltage when exposed to light. However, TiO_2 is transparent for visible light due to wide band gap. Therefore, the conversion efficiency was low when the sun was used as an illumination source. Nowadays, ZnO, which is a metal oxide material with direct band gap (3.37 eV) and crystallized in hexagonal wurtzite structure, is used as an alternative material instead of TiO_2. Due to its large bandgap, ZnO is an excellent semiconductor material such as GaN and SiC, as well as other wide-band materials. The band gap value of ZnO materials is very close to TiO_2. In addition, electron mobility and electron diffusion coefficient of DSSC application is very important. If we compare these values for both materials, the electron mobility (205–300 $cm^2V^{-1}s^{-1}$ for bulk ZnO) and electron diffusion coefficient (5.2 cm^2s^{-1} for bulk ZnO) of ZnO are higher than the electron mobility (0.1–4 $cm^2V^{-1}s^{-1}$ for bulk TiO_2) and electron diffusion coefficient (0.5 cm cm^2s^{-1} for bulk TiO_2) of TiO_2 [1]. Due to these outstanding features of ZnO, ZnO-based DSSC technology is being extensively explored. R. Vittal and K. Chuan Ho [3] compared ZnO and TiO_2 as semiconductor material, in DSSCs, in their review and they stated that ZnO is the closest alternative to TiO_2. The authors also stated that the performance of a ZnO-based DSSC is closely related to the dye used and the parameters used in the dye.

In the literature, techniques such as solution composition [4], hydrothermal [5,6], sol-gel method [7], spraying [8], microwave

* Corresponding author.
E-mail address: mcaglar@eskisehir.edu.tr (M. Caglar).

https://doi.org/10.1016/j.molstruc.2019.04.040
0022-2860/

assisted hydrothermal (MW-HT) [9,10] are used to obtain ZnO nanopowder. Among these methods, MW-HT has many advantages. Due to its unique properties, such as energy saving, short reaction time, advanced reaction selectivity, rapid volumetric heating and high product yield, the synthesis of ZnO nanoparticles by MW-HT method is rapidly increasing.

Many factors affect the performance of DSSC, such as the morphology and thickness of the electrode and the type of dye. In order to increase DSSC yield, many studies have been done based on changing ZnO morphology and thickness. Although DSSCs are manufactured successfully, another problem is the dye loading process. It usually takes a few hours. There are only a few studies working the effect of dye loading time on DSSC performance. Some researchers also investigated the effect of dye loading time on conversion efficiency ($n\%$) [11,12]. One of these studies [11] was published by A. Singh et al. In the study, they used N719 dye to form the dye solution. They investigated the effects of different dye loading times (6 h and 12 h) on energy conversion efficiency. They reported that energy conversion efficiency increased from 0.38% to 0.44% depending on the increased dye loading times. Similarly, S. S. Khadtare et al. [12] fabricated ZnO based DSSC and investigated the effect of dye loading time (5, 14 and 20 h) on energy conversion efficiency. The authors used Lawsone, the dye that was extracted from the henna, in their work and the reported energy conversion efficiencies are 0.22%, 0.19% and 0.51% for 5 h, 14 h and 20 h, respectively. As shown from the results, the dye loading for 20 h allowed them to achieve the highest power conversion efficiency.

For this reason, in our study, the effect of both dye loading time and stand-by time stability on the performance of ZnO-DSSCs has been investigated. Firstly, ZnO films were obtained by doctor blade method using ZnO nanopowders synthesized by MW-HTS method and then it was successfully applied as photoanode for the fabrication of DSSCs. The phases and morphologies of both ZnO nanopowders and films were investigated using X-ray diffraction (XRD) and scanning electron microscopy (SEM), respectively. The optical band gap values of the ZnO films with and without dye were also compared to each other. The short current (I_{sc}), open circuit voltage (V_{oc}), conversion efficiency ($n\%$) and fill factor (FF) values of ZnO-DSSCs were determined. ZnO DSSCs were kept for different (1–3) day to test the efficiency and the measurements were repeated.

2. Experimental details

2.1. Deposition of ZnO nanopowder

ZnO nanopowders were synthesized by microwave assisted hydrothermal (MW-HT) method. For this, the aqueous solutions of zinc acetate dihydrate (ZnAc; 0.15 M) and sodium hydroxide (NaOH; 4 M) were prepared as precursor materials. The solutions were stirred for 20 min at room temperature in a magnetic stirrer and then placed in a microwave oven (CEM Mars 6). These solutions were irradiated with microwaves at 300 W for 10 min. The precipitates formed after the microwave process were filtered and washed with washed with deionized water and ethanol for several minutes. The final nanopowders were dried in an oven at 60°C for 24 h and then calcined in air at 500°C for 2 h.

2.2. DSSC fabrication

Fluorine-doped tin oxide (FTO) substates to be spread onto ZnO paste were firstly cleaned in ultrasonic bath of acetone solution for 15 min and then rinsed with distilled water. And then, the substrates dried at nitrogen ambiant. The ZnO paste was prepared by mixing the ZnO nanopowder, Triton-X 100 and acetyl acetone. The resulting pastes were spread onto the FTO glass by doctor-blade method. In this process, the ZnO film was prepared by squeezing the paste onto the FTO substrate using plastic tapes and then it was annealed for 1 h at 400°C in air and then cooled. The thickness of the ZnO film is about 4.5 μm. And then, The ZnO films were immersed into a 0.5 mM N719 (ruthenizer 535 bis-TBA, Solaronix) for 1 and 2 h. Later, the dye loaded ZnO films on FTO substrate were assembled by fixing with Pt counter electrode to form a sandwich-type DSSCs. Finally, iodide/tri-iodide redox couple electrolyte (Iodolyte Z, Solaronix) was injected into the DSSC. The active area of the DSSC was about 0.36 cm^2. The solar cells loaded in the dye for 1 and 2 h were named ZnO-DSSC1 and ZnO-DSSC2, respectively. The schematic diagram of ZnO-DSSC is given in Fig. 1.

2.3. Characterization of ZnO and DSSCs

BRUKER D2 PHASER CuKα X-ray powder diffractometer was used to determine the crystalline nature, crystallite size and phase purity of ZnO film and powder. For surface morphology studies of ZnO powder and film, ZEISS Ultraplus SEM was used. SCHIMADZU UV spectrophotometer was used for reflectance measurements. The current–voltage (I–V) characteristics of the ZnO-DSSCs were recorded by a solar cell measurement system (FYTRONIX OPTOSENSE).

3. Results and discussion

XRD, a powerful and non-destructive technique, is used to characterize crystal materials. XRD spectra provide information on structural parameters such as crystal orientations, average grain size, crystallinity and crystal defects. XRD spectra for ZnO powder and film as a function of diffraction angle θ are taken by using an X-Ray powder diffractometer, and shown in Fig. 2. The XRD pattern of the ZnO film is no different from the powder. Both are highly crystallized in the hexagonal wurtzite structure (JCPDS No. 0036–1451). The basic five peaks of ZnO are found in both spectra. The interplanar spacings (d) and diffraction peaks belong to *(100)*, *(002)*, *(101)*, *(102)* and *(110)* planes are well matched to the standard diffraction pattern of wurtzite ZnO (JCPDS reference 36–1451). The 2θ and d values are given in Table 1. The crystallite

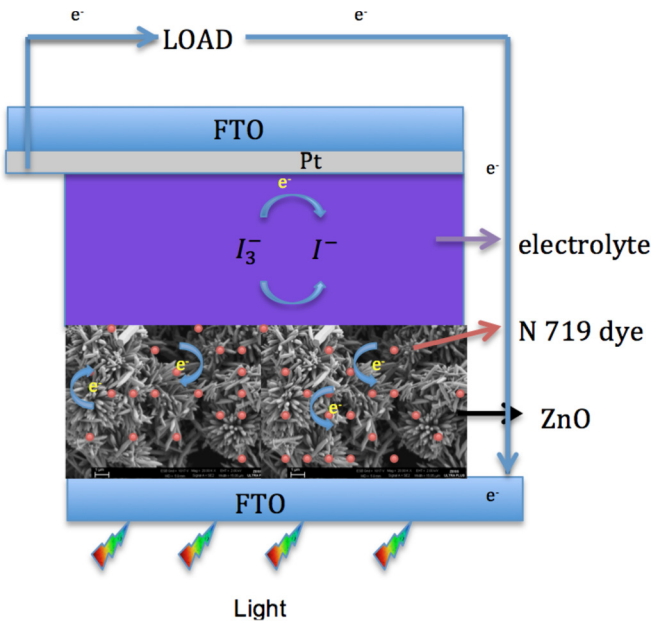

Fig. 1. Schematic representation of a DSSC based on ZnO nanostructure.

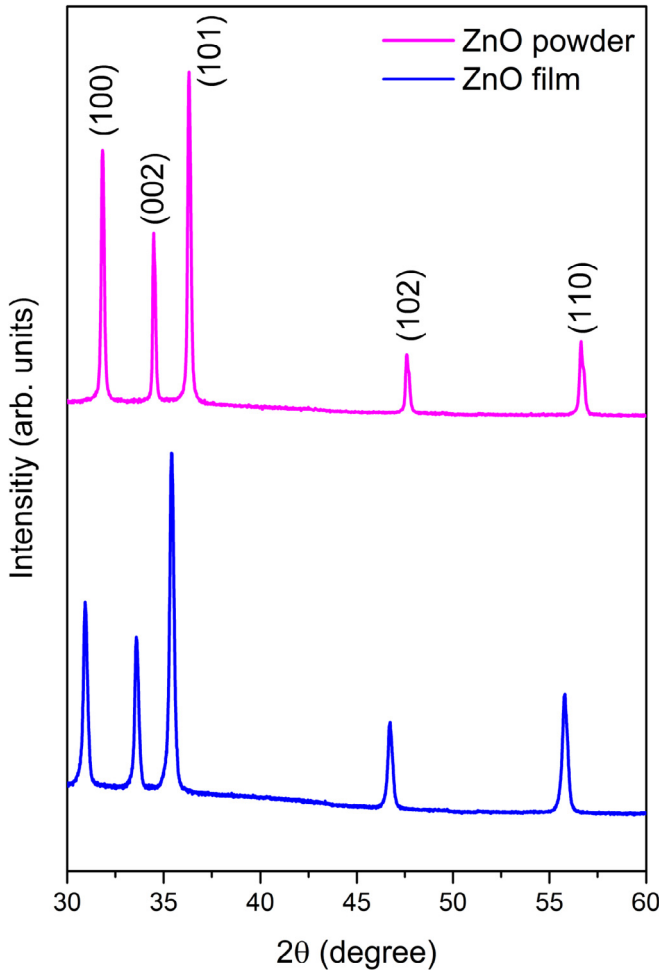

Fig. 2. XRD spectra of the ZnO film and powder.

Table 1
Structural parameters of the ZnO film and powder.

	(h k l)	2θ(*degree*)	D (Å)	D (nm)
Powder	(100)	31.041	2.88101	
	(002)	33.706	2.65911	
	(101)	35.527	2.52687	**34**
	(102)	46.836	2.80752	
	(110)	55.898	1.64487	
Film	(100)	31.095	2.87616	
	(002)	34.507	2.81111	
	(101)	36.325	2.47320	**46**
	(102)	47.616	1.90978	
	(110)	**56.657**	**1.62461**	

size of the ZnO powder and film were calculated using the Scherrer Equation [13] and is given in Table 1. As seen in Table 1, the crystallite size calculated for ZnO film is larger than that of calculated for the powder. This difference between the film and the powder of ZnO may be caused by the annealing process applied at 400 °*C* after the film formation.

Fig. 3 shows the SEM images of ZnO powder and film that were taken at different magnifications. The highly dense and uniform flower like morphology of the ZnO powder is seen in Fig. 3(a). The length of rods formed flower like stucture has about 2 μm and diameter is 200 nm. The image of ZnO film is shown in Fig. 3(b). As seen from this figure, there is no change in the morphological structure of ZnO after the film is formed.

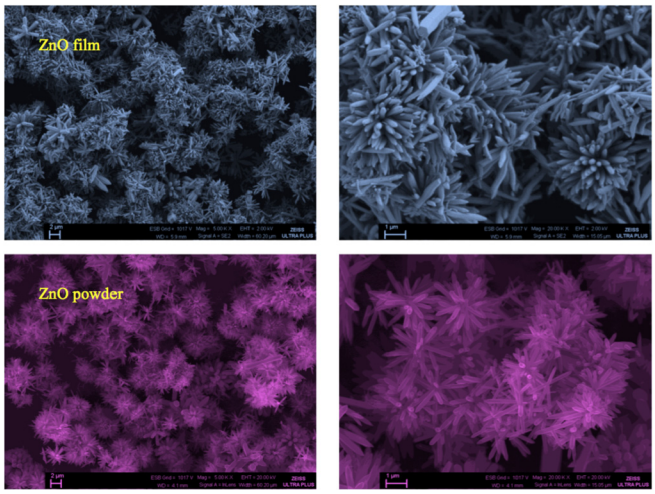

Fig. 3. SEM images of the ZnO film and powder.

In Fig. 4, the absorption spectra of the without and dyes loaded ZnO films are illustrated. As shown in this figure, the absorbance values increase as the dye loading time increases in 400–800 nm region. The loaded time of 2 h was sufficient for the dye to be adsorbed onto the ZnO surface. The absorption spectrum of the dye loaded ZnO shows a broad peak around 500 nm, corresponding to the π–π^* orbital transition, and the intensity of 2 h loaded one is higher than that of 1 h.

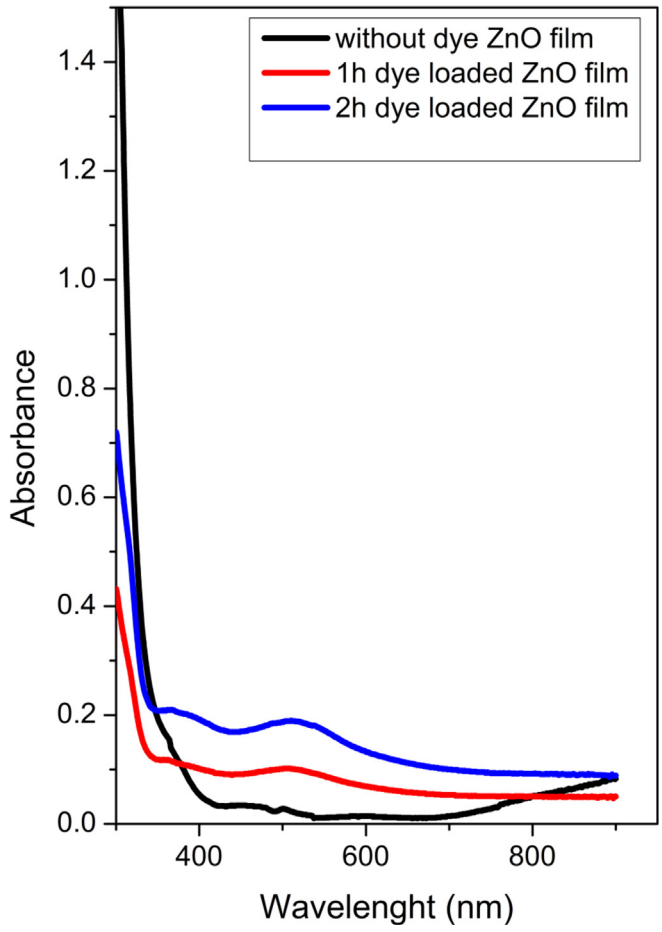

Fig. 4. Absorbance spectra of the bare and dye loaded ZnO film.

The optical reflectance measurements, which were carried out at room temperature by using a BaSO4 powder as reference, were used to determine the optical band gap of the ZnO film. The band gap values of ZnO film were determinde by the use of Kubelka-munk function. Kubelka Munk function F(R) [14],

$$\frac{K}{S} = \frac{(1-R)^2}{2R} = f(R) \quad (1)$$

where K is absorption coefficient and S is scattering coefficient. In order to calculate the band gap, the reflection values must be converted to absorbance using the Kubelka-Munk function. The above equation was changed and rewritten with the relationship given below

$$\left(\frac{F(R)h\nu}{d}\right)^2 = A(h\nu - E_g) \quad (2)$$

where E_g is the optical band gap, d is the film thickness, A is the constant and $h\nu$ is the photon energy. The diffuse reflectance spectra of without dye and dye loaded ZnO film are given in Fig. 5. The bare ZnO film has an average reflectivity of 70% in the UV region. Therefore, ZnO's superior light-scattering ability is high. This shows that the ZnO film is well crystallized. It is also shown that the reflectance value of the ZnO film decreases with increasing dye loading.

The optical band gap values of without dye and dye loaded ZnO film were determined from the point that cuts the energy axis of the linear part of the graph given in Fig. 6. This graph are characterised by the presence of two bands. The band at approximately 3.25 eV in each of the three spectra corresponds to the optical band

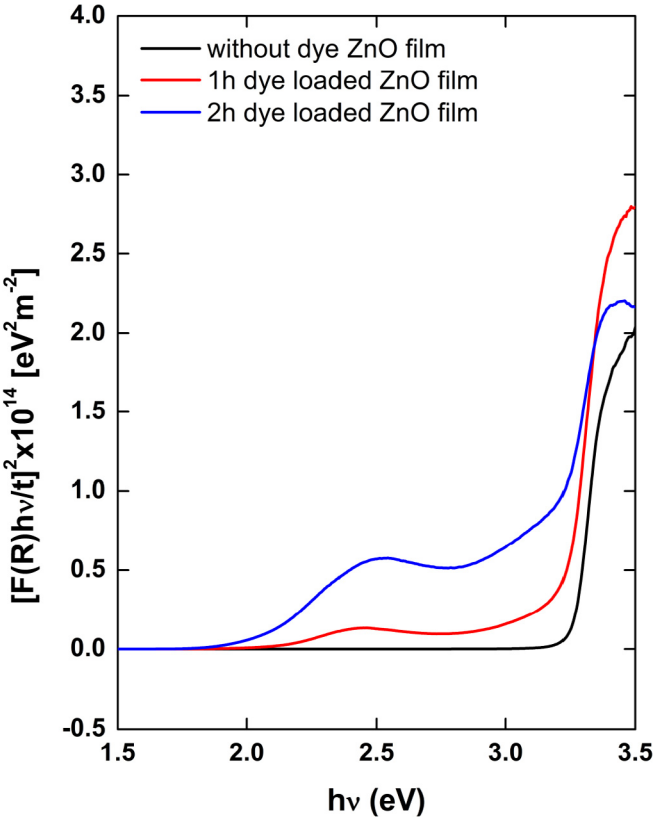

Fig. 6. Kubelka munk function of bare and dye loaded ZnO film.

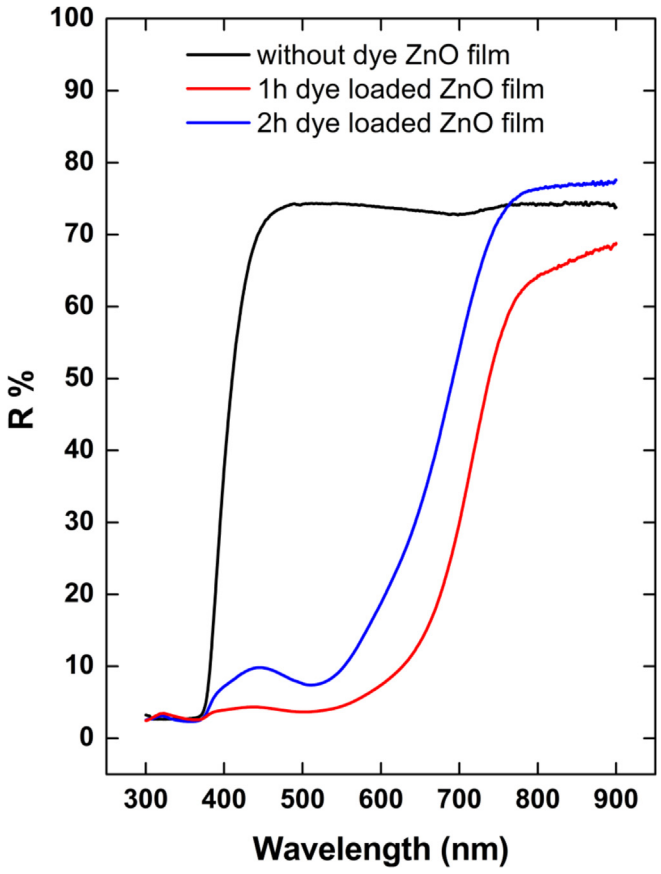

Fig. 5. Reflectance spectra of the bare and dye loaded ZnO film.

gap of ZnO. The other band located in the 2.20 eV is associated with the high-energy $\pi-\pi^*$ orbital transition which belongs to the ruthenium. Based on these results, it is proposed that the ruthenium complex was excited to the metal to ligand charge transfer (MLCT) excited state, from which an electron is injected directly to the ZnO conduction band [15].

The energy band diagram of DSSC which includes HOMO/LUMO levels of N719 dye, conduction band (CB) and valence band (VB) of ZnO, the work function of FTO and reduction potential of the electrolyte is illustrated schematically in Fig. 7. As seen in this figure, the CB and VB energy levels of ZnO are lower than the LUMO

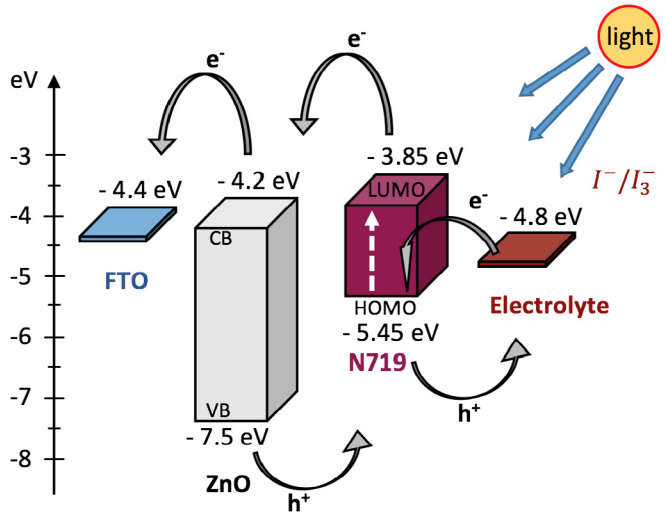

Fig. 7. Schematic energy band diagram for FTO, ZnO and N719 dye.

and HOMO energy levels of the N719 dye. Therefore, the photogenerated electrons in dye can be collected from ZnO and transferred rapidly to the FTO.

Several photovoltaic parameters can be derived from *I–V* curves of DSSC. When the voltage applied on the cell is 0 V, the measured current is the short circuit current (I_{SC}). The maximum measured voltage is the open circuit voltage (V_{oc}) while no current flows through the circuit. The fill factor (FF) is a measure of the quality of the cell as a power source. It is the ratio of maximum power to open circuit voltage and short circuit voltage circuit current multiplication. The general formula for the FF is:

$$FF = \frac{I_{max} x V_{max}}{I_{sc} x V_{oc}} \quad (3)$$

The power conversion efficiency ($n\%$) is the ratio between maximum generated power (P_{max}) and electrical input power (P_{in}) from the light source and found to be following equation

$$n(\%) = \frac{FF x I_{sc} x V_{oc}}{I_{max} x V_{max}} x100 \quad (4)$$

The current density-voltage (*J-V*) graphs obtained for ZnO-1-DSSC and ZnO-2-DSSC are shown in Fig. 8 and Fig. 9. From the *J-V* graphs, DSSC parameters such as V_{oc}, J_{sc}, *FF* and $n\%$ values are estimated using Equations (3) and (4) [16] and given in Table 2. It can be seen in these figures that the dye loading time and standby time have an important effect on the photovoltaic performance of the DSSCs. As shown in Table 2, the J_{SC} and $n\%$ values are in similar trend with dye loading time for both ZnO-DSSCs. Also, the V_{oc} tends to increase when increasing the dye loading time to the highest value. The highest conversion is the conversion of ZnO-DSSC2-2 and also the ideal dye loading time was optimized to be 2 h. While an increment in efficiency in ZnO-DSSC-1 was observed in measurement performed after 1 day standby time in the case of 1 h loading time in the dye, similar increase for the ZnO-DSSC-2 having 2 h loading time was observed in measurement performed 2 days later.

There are some factors such as crystal structure, energy gap, morphology, porosity, surface area and number of film layers that affect the efficiency of photovoltaic cells. In addition, the factors such as film thickness and dye loading time also affect the conversion efficiency. In general, if the film thickness is fixed, photovoltaic performance increases with increase dye loading time. However, the dye loading time causes a decrease in performance due to dye agglomeration after a while [17]. That is, the observed decrease in the conversion efficiency values after an optimum loading time can be a result of both the deterioration of the semiconducting film and the presence of aggregates in the pores.

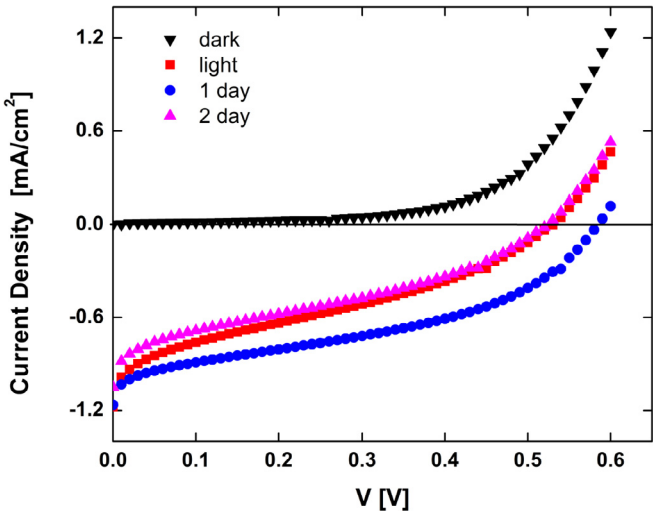

Fig. 8. *J-V* graph of ZnO-DSSC-1.

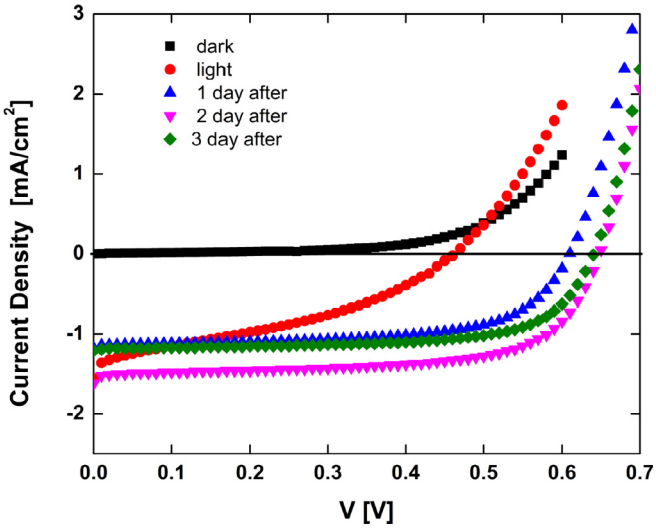

Fig. 9. *J-V* graph of ZnO-DSSC-2.

Table 2
The photovoltaic parameters of ZnO-DSSCs.

DSSC	V_{oc} (V)	J_{sc} (mA/cm^2)	*FF*	$n\%$
ZnO-DSSC1	0.53	1.18	0.25	0.16
ZnO-DSSC1-1	0.58	1.16	0.35	0.25
ZnO-DSSC1-2	0.52	1.05	0.28	0.14
ZnO-DSSC2	0.46	1.55	0.32	0.23
ZnO-DSSC2-1	0.61	1.18	0.62	0.44
ZnO-DSSC2-2	0.64	1.62	0.62	0.64
ZnO-DSSC2-3	0.64	1.21	0.66	0.51

4. Conclusions

The crystal structure and surface morphologies of both ZnO nanopowders synthesized by MW-HT method and obtained films using these powders were investigated and these results showed us the highly crystallized hexagonal stucture and nanoflower structures decorated with rods. The optical band gaps of the ZnO films were evaluated by using Kubelka-Munk function and two optical band gaps were detected at about 3.25 eV and 2.20 eV associated with ZnO and ruthenium. As a result of electrical measurements of ZnO-DSSCs fabricated by using dye solution consisting N719 performed under 100 mW/cm^2 simulated sunlight, it was determined that the performance of the ZnO-DSSCs depend on both loading time and standbye time. The best performance was obtained for 2 h loading time and 2 days standby time. This cell performed with the highest short-circuit density of 1.62 mA/cm^2; efficiency of 0.64%; open circuit voltage of 0.64 V and fill factor of 0.62.

Acknowledgements

This work was supported by Eskisehir Technical University Commission of Scientific Research Projects under Grant No. 1706F385.

References

[1] A.P. Uthirakumar, Fabrication of ZnO Based Dye Sensitized Solar Cells, InTech, 2011.

[2] B. O'Regan, M. Grätzel, A low-cost, high-efficiency solar-cell based on dye-sensitized colloidal TiO_2 films, Nature 353 (1991) 737–740.

[3] R. Vittal, K. Ho, "Zinc oxide based dye-sensitized solar cells : a review, Renew. Sustain. Energy Rev. 70 (2017) 920–935. March 2016.

[4] S. Park, S.Y. Park, W.J. Park, H. Lim, S. Lee, J. Lee, Effects of heat-treatment on photoluminescence spectra and photocatalytic properties of solution-combusted ZnO nanopowders, J. Nanosci. Nanotechnol. 19 (3) (2019) 1764–1767.

[5] S.D. Senol, O. Ozturk, C. Terzioğlu, Effect of boron doping on the structural, optical and electrical properties of ZnO nanoparticles produced by the hydrothermal method, Ceram. Int. 41 (9) (2015) 11194–11201.

[6] D. Li, J. Yao, H. Sun, B. Liu, S. Agtamaal, C. Feng, Recycling of phenol from aqueous solutions by pervaporation with ZSM-5/PDMS/PVDF hollow fiber composite membrane, Appl. Surf. Sci. 427 (2018) 288–297.

[7] B. Liu, H.C. Zeng, Hydrothermal synthesis of ZnO nanorods in the diameter regime of 50nm, J. Am. Chem. Soc. 125 (2003) 4430–4431.

[8] S. Rani, P. Suri, P.K. Shishodia, R.M. Mehra, Synthesis of nanocrystalline ZnO powder via sol-gel route for dye-sensitized solar cells, Sol. Energy Mater. Sol. Cells 92 (12) (2008) 1639–1645.

[9] A.S. Manikandan, K.B. Renukadevi, K. Ravichandran, P.V. Rajkumar, K. Boubaker, Enhanced photocatalytic, antibacterial and magnetic properties of ZnO nanopowders through lattice compatible cobalt doping, J. Mater. Sci. Electron. 27 (11) (2016) 11890–11901.

[10] Y. Caglar, K. Gorgun, S. Aksoy, "Effect of deposition time on the properties of ZnO nanopowder prepared by microwave-assisted hydrothermal synthesis, in: 2014 10th International Vacuum Electron Sources Conference, IVESC 2014 and 2nd International Conference on Emission Electronics, ICEE 2014 - Proceedings, 2014.

[11] A. Singh, D. Mohan, D.S. Ahlawat, Richa, Influence of dye loading time and electrolytes constituents ratio on the performance of spin coated zno photoanode based dye sensitized solar cells, Orient. J. Chem. 32 (2) (2016) 1049–1054.

[12] S.S. Khadtare, S.R. Jadkar, S. Salunke-Gawali, H.M. Pathan, Lawsone sensitized ZnO photoelectrodes for dye sensitized solar cells, J. Nano Res. 24 (2013) 140–145.

[13] B.D. Cullity, Elements of DIFFRACTION, 1978.

[14] F. Kubelka, P. Munk, Ein Beitrag zur optik der farbanstriche, Z.Tech. Phys. (Leipzig) 12 (1931) 593–601.

[15] K. Awasthi, H.Y. Hsu, E.W.G. Diau, N. Ohta, Enhanced charge transfer character of photoexcited states of dye sensitizer on the N719/TiO2 interface as revealed by electroabsorption spectra, J. Photochem. Photobiol. A Chem. 288 (2014) 70–75.

[16] T. Marimuthu, N. Anandhan, R. Thangamuthu, S. Surya, Influence of solution viscosity on hydrothermally grown ZnO thin films for DSSC applications, Superlattice. Microst. 98 (2016) 332–341.

[17] O. Wiranwetchayan, P. Ruankham, W. Promnopas, S. Choopun, P. Singjai, A. Chaipanich, S. Thongtem, Effect of nanoporous In2O3 film fabricated on TiO2-In2O3 photoanode for photovoltaic performance via a sparking method, J. Solid State Electrochem. 22 (8) (2018) 2531–2543.